PHYSICS AND CHEMISTRY OF SOLID STATE

V. 26, No. 2 (2025) pp. 312-321

Section: Physics

DOI: 10.15330/pcss.26.2.312-321

Vasyl Stefanyk Precarpathian National University

ФІЗИКА І ХІМІЯ ТВЕРДОГО ТІЛА Т. 26, № 2 (2025) С. 312-321

Фізико-математичні науки

PACS: 75.75.-c, 75.30.Cr, 82.70.-y, 87.85.Rs

ISSN 1729-4428 (Print)
ISSN 2309-8589 (Online)

J. Mazurenko^{1,2}, L. Kaykan¹, V. Moklyak^{1,3}, M. Moklyak⁴, M. Moiseienko⁵, N. Ostapovych⁵, M. Petryshyn⁶

Inductive Heating Behavior of Copper Ferrite Magnetic Nanoparticles

¹Laboratory for Physics of Magnetic Films № 23, G.V. Kurdyumov Institute for Metal Physics, N.A.S. of Ukraine, Kyiv, Ukraine; ²Department of Magnetism, Institute of Experimental Physics SAS, Košice, Slovak Republic, <u>mazurenko@saske.sk</u>;

This study investigates the inductive heating behavior of CuFe₂O₄ magnetic nanoparticles (MNPs) for potential application in magnetic hyperthermia. CuFe₂O₄ nanoparticles were synthesized using the sol-gel autocombustion method and subjected to annealing at 400°C and 800°C to assess the effect of thermal treatment on their structural and magnetic properties. X-ray diffraction (XRD) analysis revealed a phase transition from the cubic spinel structure (Fd3m) in the as-prepared samples to a tetragonal phase (I41/amd) after annealing, with particle sizes ranging from 20 to 30 nm. Transmission electron microscopy (TEM) confirmed spherical morphology and uniform particle distribution, while vibrating sample magnetometry (VSM) measurements showed that annealing significantly influenced the saturation magnetization and coercivity, key parameters for heating performance. Specific absorption rate (SAR) and intrinsic loss power (ILP), estimated using Box-Lucas and Newton cooling models, demonstrated that the nanoparticles maintained strong heating efficiency across thermal treatments, with SAR values of ~30–32 W/g. The results suggest that CuFe₂O₄ nanoparticles are promising candidates for magnetically guided hyperthermia applications, with tunable properties that can be optimized for clinical readiness.

Keywords: Copper Ferrite, Magnetic nanoparticles, Inductive heating, Box Lucas Method, Newton Cooling Approach.

Received 03 December 2024; Accepted 08 June 2025.

Introduction

Magnetic nanoparticles have gained significant attention in recent years due to their unique magnetic [1], thermal [2], and chemical properties [3], which make them promising candidates for a wide range of technological [4] and biomedical applications [5]. Among these, magnetic hyperthermia stands out as an innovative approach for localized heating [6], particularly in cancer treatment [7], where controlled thermal energy can selectively destroy tumor cells while sparing healthy tissues. The efficiency

of this process depends not only on the external magnetic field parameters but also on the intrinsic magnetic and structural properties of the nanoparticles themselves. Copper ferrite (CuFe₂O₄) [8], a type of spinel ferrite, offers tunable magnetic characteristics and good chemical stability, making it a compelling material for inductive heating applications.

Magnetic hyperthermia [9] is an advanced cancer treatment technique that employs magnetic nanoparticles to produce localized heating when subjected to an alternating magnetic field (AMF). This localized heating leads to the targeted destruction of cancer cells.

³ Department of Physical and Mathematical Sciences, Ivano-Frankivsk National Technical University of Oil and Gas, Ivano-Frankivsk, Ukraine, <u>volodymyr.mokliak@nung.edu.ua</u>;

⁴Department of Applied Physics and Materials Science, Vasyl Stefanyk Precarpathian National University, Ivano-Frankivsk, Ukraine, <u>mariamoklyak@gmail.com</u>;

⁵Department of Medical Informatics, Medical and Biological Physics, Ivano-Frankivsk National Medical University, Ivano-Frankivsk, Ukraine, mmoiseyenko@ifnmu.edu.ua, nataost@ifnmu.edu.ua;

⁶Department of Computer Science, Vasyl Stefanyk Precarpathian National University, Ivano-Frankivsk, Ukraine. <u>m.l.petryshyn@pnu.edu.ua</u>

Commonly used materials for this procedure include iron oxide (Fe₃O₄), and other ferrites. These nanoparticles are often functionalized to enhance their stability and biocompatibility. Typically, the nanoparticles range in size from 5 to 100 nm in diameter [10 - 13].

In magnetic hyperthermia an alternating magnetic field with a specific frequency and amplitude is applied to the nanoparticles. Heat is generated through two primary mechanisms: Néel relaxation [14], which involves the reorientation of the magnetic moment within the particle, and Brownian relaxation [15], which involves the physical rotation of the entire nanoparticle in the fluid.

The primary advantage of using nanoparticles in hyperthermia is their ability to generate heat locally, increasing the temperature of the surrounding tissue to the therapeutic range of 42-45°C [16]. This temperature range selectively damages cancer cells more than normal cells due to the higher susceptibility of cancer cells to heat. Elevated temperatures induce protein denaturation [17], disrupt cellular functions [18], and increase cell membrane permeability [19], leading to loss of membrane integrity and subsequent cell lysis [20]. This precise thermal targeting enhances the efficacy of the treatment minimizing damage to healthy Hyperthermia induces heat shock proteins (HSPs) [21], which can enhance antigen presentation and stimulate an immune response against tumor cells. Increased infiltration of immune cells such as macrophages and lymphocytes are often seen in treated areas, aiding in tumor clearance.

The main aim of this article is to investigate the inductive heating behavior of copper ferrite magnetic nanoparticles and to identify the key material and magnetic parameters that optimize their heating efficiency for potential applications in magnetic hyperthermia.

I. Materials and Methods

Copper ferrite (CuFe₂O₄) nanoparticles were prepared by the sol-gel autocombustion method [22]. Iron nitrate (Fe(NO₃)₃·9H₂O), copper nitrate (Cu(NO₃)₂·3H₂O), and citric acid (C₆H₈O₇) were combined in stoichiometric amounts, with citric acid serving as fuel. The mixture was dissolved in distilled water, stirred, and the pH adjusted to 7 [23] using aqueous ammonia. After drying, the resulting gel was heated at 250–300°C, triggering a self-sustaining combustion reaction that produced porous copper ferrite powder. Samples were labelled RT (as-prepared, unannealed) and C400, and C800 according to annealing temperatures of 400°C, and 800°C, respectively.

X-ray diffraction (XRD) studies were conducted using an Empyrean PANalytical powder diffractometer (Malvern Panalytical, Malvern WR14 1XZ, UK) with Bragg—Brentano geometry. Data were collected over a 20 range from 20° to 90° with a step size of 0.033° and an acquisition time of 25 minutes per pattern, following a 20-minute temperature stabilization period.

The microstructural characterization of the nanopowders was performed using a transmission electron microscopy (TEM) FEI Tecnai G2 20 (FEI, Hillsboro, OR, USA) with a LaB6 cathode operating at acceleration voltage 200 kV.

The magnetic properties of the CuFe₂O₄ samples were characterized using a LakeShore 7407 vibrating sample magnetometer (VSM, Westerville, USA) at room temperature and during heat treatment in air.

The equipment used to assess the magnetic hyperthermic effect included a chamber designed to hold 0.4 mL of the sample. This sample was positioned in a polymer Eppendorf tube, paired with an optical fibre temperature sensor linked to a temperature recording system [24, 25]. For accurate placement and thermal insulation during heating, the sample was set at the centre of an induction coil, using a polymer supporter of 2.5 cm diameter. The magnetic field was produced by the EASY Heat 0224 FFC CE induction heating generator from St. Louis, MO, USA. A water-cooling system (TEXA TCW12NBSBCP0000, Pegognaga, Italy) was employed to maintain the induction coil's temperature. Tests were conducted by adjusting the generator's power between 0.6-1.6 kW, correlating to a magnetic field strength (H) of 23.8-35.7 kA/m; an H value of 23.8 kA/m was chosen for SAR determination.

II. Results and discussion

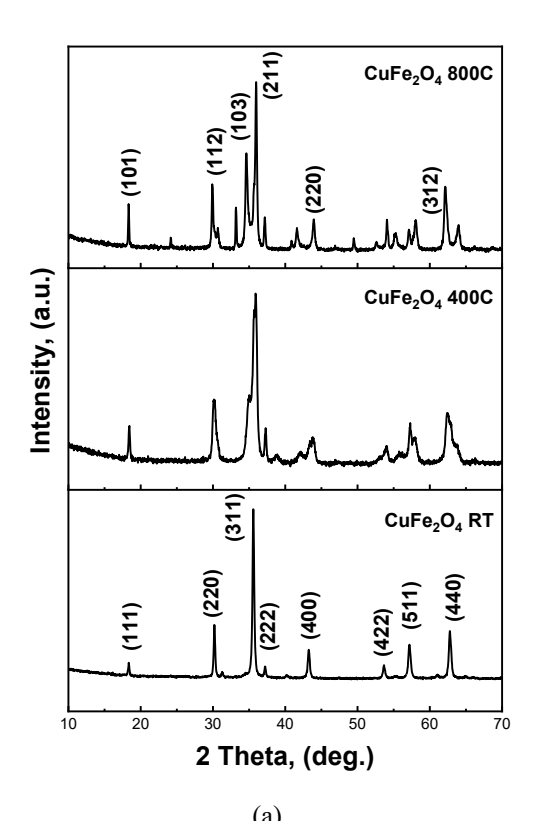
2.1. Structural Studies

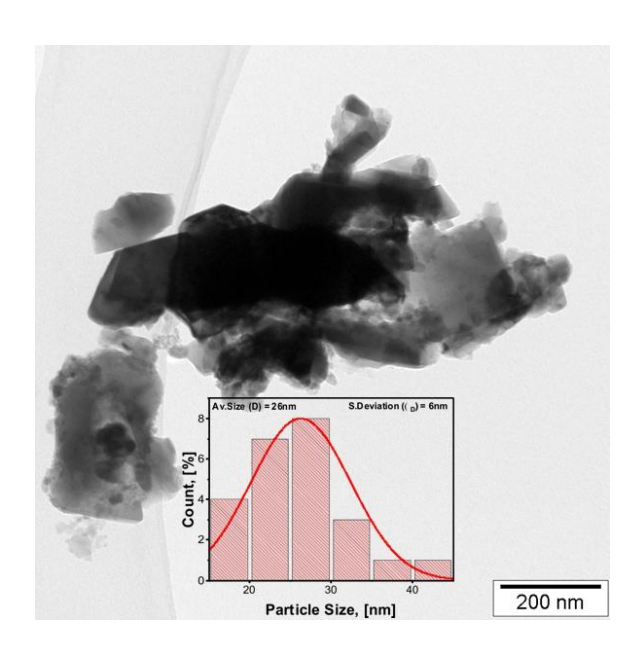
X-ray diffraction (XRD) analysis was conducted to investigate the phase composition and crystal structure of the CuFe₂O₄ nanoparticles, with results shown in Figure 1(a). The as-prepared sample exhibited diffraction peaks corresponding to the cubic spinel structure (space group Fd3m). After annealing, the diffraction pattern shifted, indicating a transition to the tetragonal phase (space group I4₁/amd), reflecting structural reorganization driven by thermal treatment. The average crystallite sizes, estimated from peak broadening using the Scherrer equation [26], were found to range between 20 and 30 nm across the samples.

Transmission electron microscopy (TEM), Figure 1(b), was used to examine the morphology and size distribution of the synthesized CuFe₂O₄ nanoparticles, with representative images shown in Figure 1 (b). The TEM analysis revealed predominantly spherical particles with relatively uniform size distributions, confirming successful synthesis. The average particle size was consistent across samples, with slight growth observed after annealing, reflecting the influence of thermal treatment on particle coarsening and crystallinity. These structural observations complement the magnetic measurements, helping to explain the variations in SAR performance with annealing.

2.2. Magnetic Studies

The vibrating sample magnetometry (VSM) measurements (Figure 2) reveal how annealing temperature affects the magnetic properties of $CuFe_2O_4$ nanoparticles. The saturation magnetization (M_S) increases markedly from 23.39 emu/g for not annealed sample to 58.01 emu/g after annealing at 400°C, indicating enhanced magnetic ordering and crystallinity. However, at 800°C, M_S decreases to 37.85 emu/g, likely due to particle growth, surface effects, or partial phase changes. Coercivity H_C steadily increases with annealing,





(b)

Fig. 1. (a) XRD diffraction patterns of CuFe₂O₄ samples, as-prepared and annealed at 400°C and 800°C; (b) TEM image of CuFe₂O₄ sample.

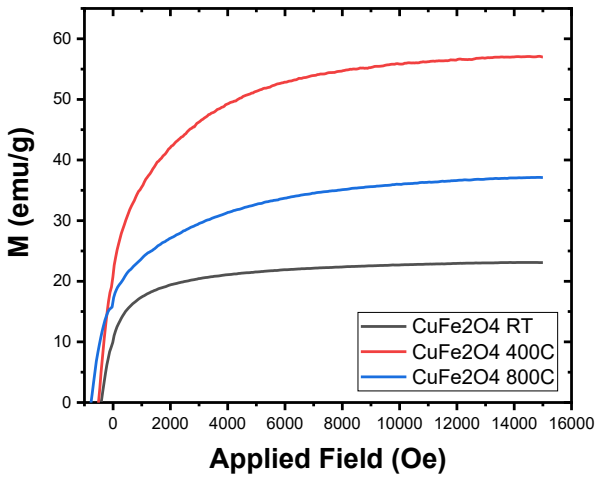


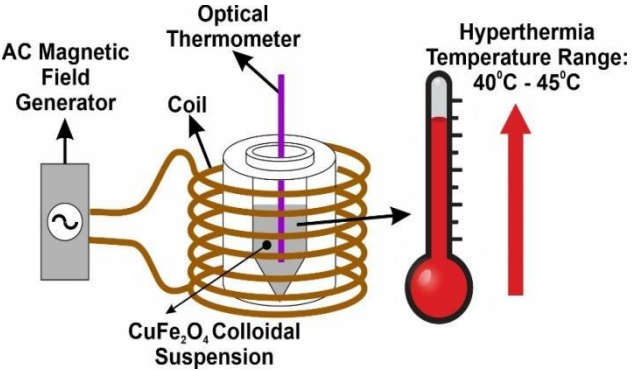
Fig. 2. VSM magnetization curves of CuFe₂O₄ nanoparticles.

from 415.5 Oe (RT) to 768.1 Oe (800°C), reflecting changes in magnetic anisotropy and domain structure [27].

2.3. Inductive Heating Studies

The heating abilities of the CuFe₂O₄ samples were evaluated using heat-response curves in a magnetic field. Figure 3 presents the experimental heat-response curves of CuFe₂O₄ (non-annealed, and annealed at 400°C, and 800°C) colloidal nanoparticles, tested under an alternating magnetic field of 23.8 kA/m and 357 kHz (scheme 1).

Each of these samples was assessed at a concentration of 1 mg/L [28]. To reproduce a tissue-like setting, the samples were dispersed within an agar matrix. Research indicates that an agar concentration of up to 4 wt%



Scheme 1. General scheme of magnetic induction heating process.

exhibits porosity and density akin to soft tissue [29]. Therefore, this study employed an agar concentration of 2wt%, emulating the properties of soft tissues. The preparation of these agar-encased emulsion samples adhered to the methodology outlined by Serantes et al. [30]. Initially, the sample was placed in a hot water-bath sonicator at 70°C for 10 minutes. Subsequently, 4 mg of agar (sourced from Sigma-Aldrich) was integrated into the emulsion, ensuring a final agar concentration of 2 wt% without altering the emulsion's concentration. This agarinfused liquid sample underwent an additional 60 minutes of sonication to achieve a uniform dispersion. This mixture was then swiftly transferred to a specially designed sample holder situated at the core of an electromagnet. It was imperative to maintain a consistent sample volume across all tests to ensure the accuracy of the SAR measurements.

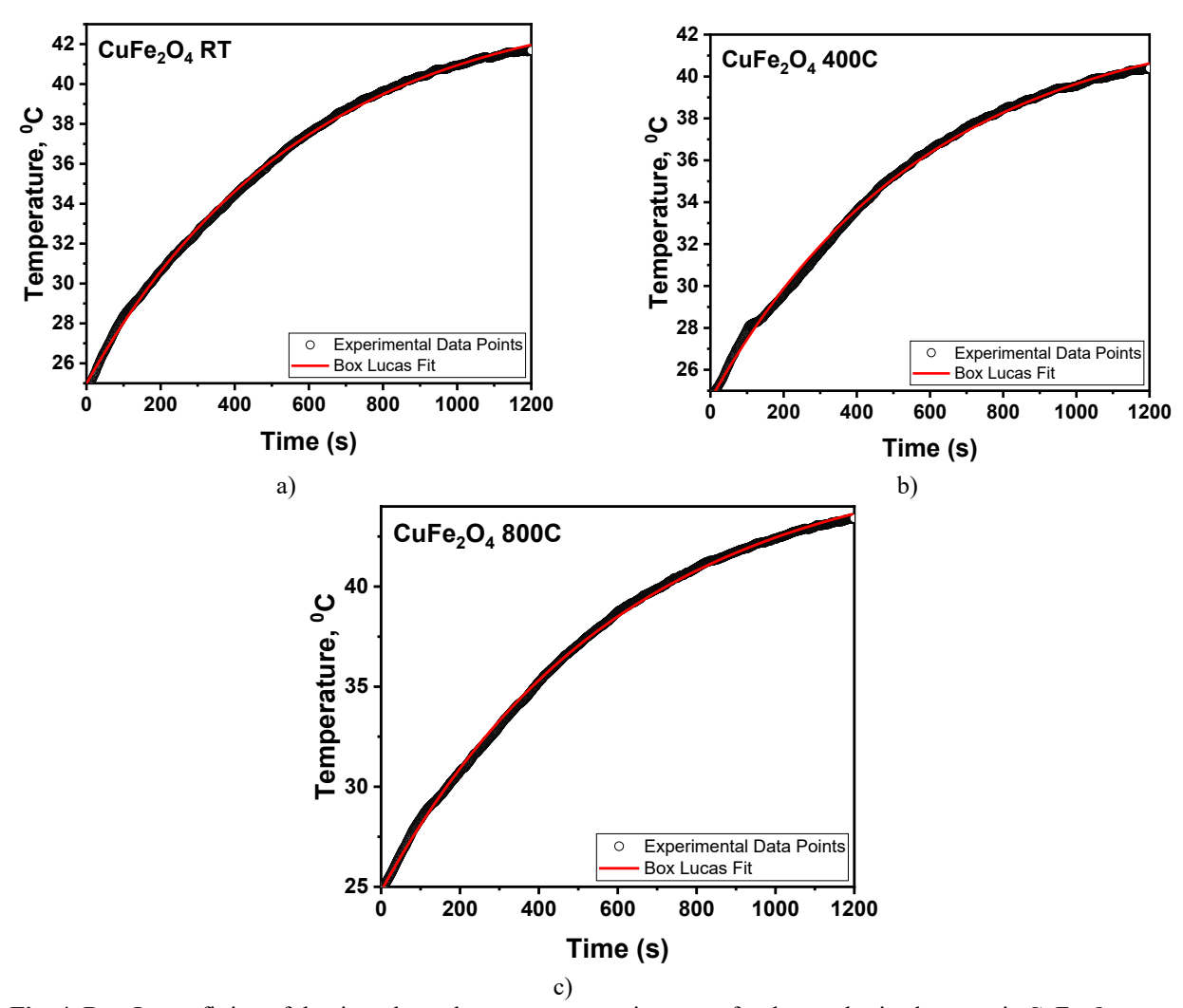


Fig. 4. Box-Lucas fitting of the time-dependent temperature rise curve for the synthesized magnetic CuFe₂O₄ nanoparticles, RT and annealed at 400°C, and 800°C, measured under 23.8 kA/m and 357 kHz alternate magnetic field.

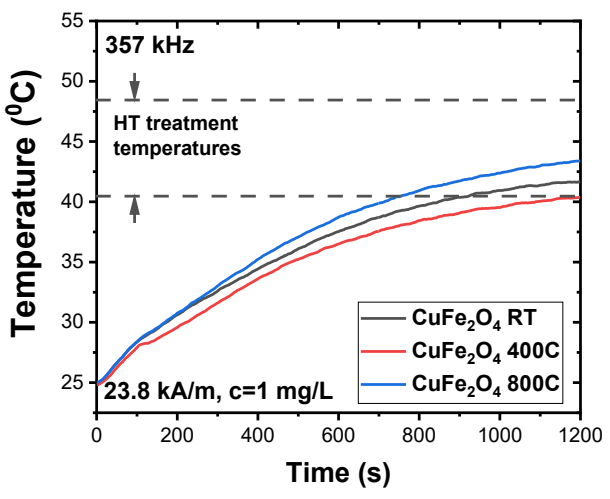


Fig. 3. Heating response curves of CuFe₂O₄ (RT and annealed at 400°C and 800°C) colloidal nanoparticles measured under 23.8 kA/m and 357 kHz alternate magnetic field.

2.3.1. Box Lucas Method

Once the magnetic material's temperature stabilizes, the temperature rise curve is fitted using the Box-Lucas approach. This method is non-adiabatic and relies on Newton's law of cooling principles. The Box-Lucas method (Figure 4) is used to determine the Specific Absorption Rate (SAR) using the following equation [31-33]

$$T(t) = a[1 - exp(-b(t - t_0))]$$
 (1)

in this context, (t₀) represents the initial time offset (20 seconds), while (a) and (b) are parameters derived from fitting the Box-Lucas equation to the experimental data. The SAR is then calculated using the expression:

$$SAR_{Box-Lucas} = \frac{M_S}{M_n} \times C(a \times b)$$
 (2)

where C is the specific heat capacity of the medium (for 2 wt% agar solution $C = 4.13 \text{ J g}^{-1}C^{-1}$), M_S is the mass of suspension (i.e. 1.5g), and Mn is the mass of the nanoparticles in the suspension (i.e. 0.01g).

Table 1. Specific absorption rate (SAR), intrinsic loss power (ILP), of RT-CuFe₂O₄ nanoparticles, annealed at 400°C, and 800°C, obtained from Box-Lucas Fit and Newton Cooling Approach Fit.

	Box-Lucas Fit			Newton Cooling Approach Fit	
Sample	SAR, W/g	ILP, nH·m²/kg	SAR, W/g	ILP, nH·m²/kg	
CuFe ₂ O ₄ RT	31.43	0.155	20.67	0.102	
$CuFe_2O_4$ 400C	30.21	0.149	19.42	0.096	
$CuFe_2O_4$ 800C	31.79	0.157	22.38	0.111	

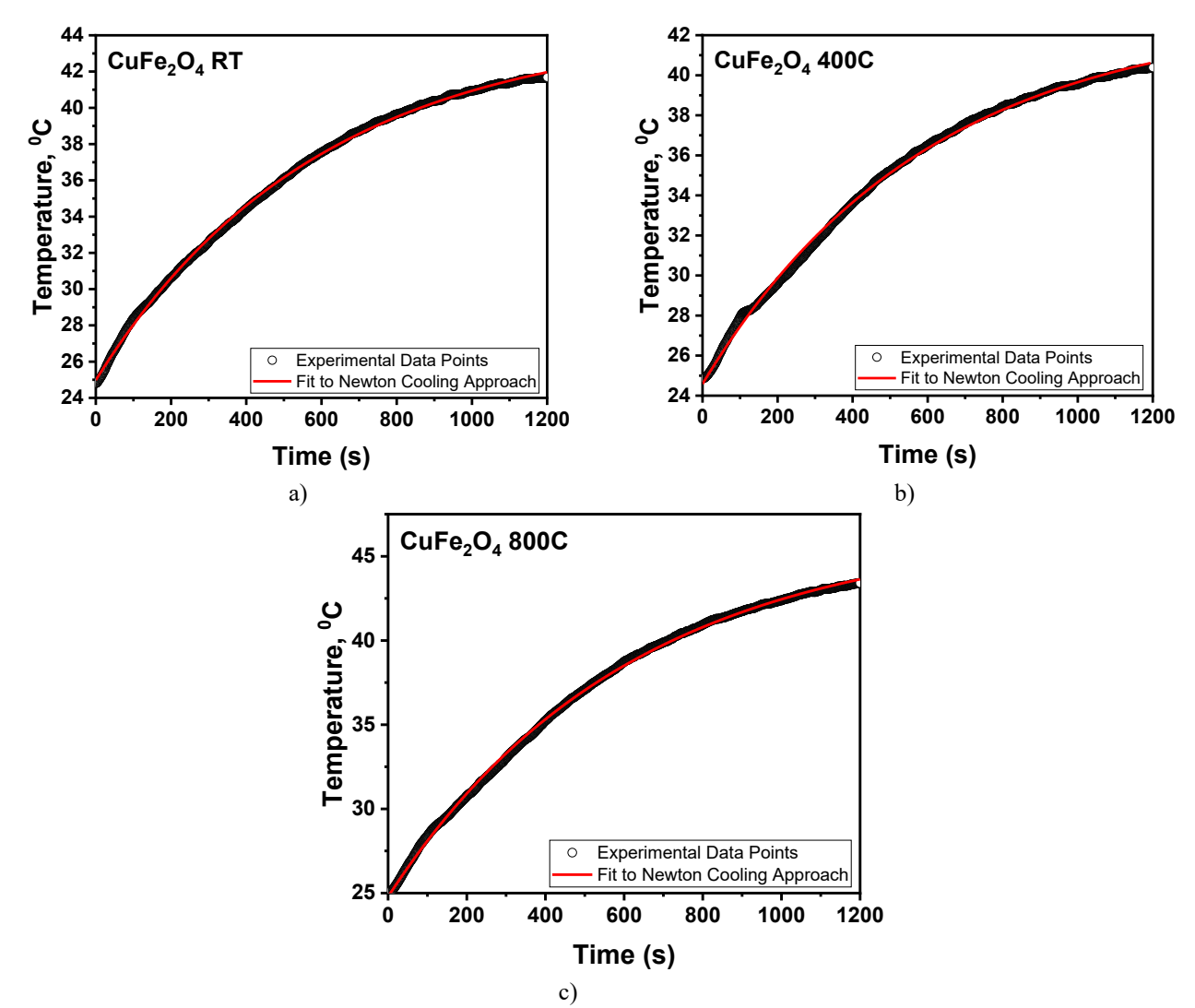


Fig. 5. Fit to the Newton Cooling Approach of the time-dependent temperature rise curve for the synthesized magnetic CuFe₂O₄ nanoparticles, RT and annealed at 400°C, 500°C, 600°C, and 800°C, measured under 23.8 kA/m and 357 kHz alternate magnetic field.

Intrinsic Loss Power [34]

$$ILP = \frac{SAR}{H^2 f} \tag{3}$$

where H is the field strength in kA/m, f is the frequency in kHz, and SAR should be substituted in W/kg.

The SAR value derived from the Box-Lucas model is listed in table 1.

2.3.2. Newton Cooling Approach Method

According to Newton's Law of Cooling, the change in temperature of a sample over time t when exposed to an alternating magnetic field under non-adiabatic conditions can be described by the following equation [35, 36],

Table 2.

Summary of main hyperthermia methods

Hyperthermia Method	Motivations	Limitations	Applications
Magnetic hyperthermia	Localized heating; non- invasive; precise targeting using magnetic nanoparticles and AMF	Limited penetration depth of AMF; nanoparticle biocompatibility and delivery challenges	Cancer treatment (glioblastoma, prostate) [37], thermally triggered drug release.
Radiofrequency (RF) hyperthermia	Deep tissue heating; suitable for large tumors; non-invasive	Non-specific heating; potential overheating of healthy tissues; complex field control	Treatment of deep-seated tumors [38] (liver, cervix [39], prostate [40, 41]).
Microwave hyperthermia	Rapid heating; effective for superficial and moderately deep tumors	Limited penetration depth; uneven heating due to tissue heterogeneity	Breast cancer [42], head and neck tumors [43], superficial lesions [44].
Ultrasound hyperthermia	Focused deep tissue heating; non-invasive; precise control with imaging guidance	Requires precise targeting; acoustic scattering and absorption in bone and air	Prostate cancer [45], brain tumors [46], uterine fibroids [47], targeted drug delivery [48].
Photothermal therapy	High spatial resolution; uses light-absorbing nanoparticles or dyes	Limited light penetration in deep tissues; requires optical window matching	Skin cancer [49], superficial tumors [50], antibacterial treatments [51], biofilm disruption [52].

$$T = T_0 + \Delta T_{max} \left[1 - exp\left(\frac{-t}{\tau}\right) \right] \tag{4}$$

The complete time-dependent temperature curve has been fitted to equation (17). The fitting parameters obtained from this process (Figure 5), specifically the maximum temperature increase ΔT_{max} and the time constant τ , are then used to calculate the SAR value using the following expression,

$$SAR = \frac{C\Delta T_{max}}{\tau} \left(\frac{m_{sample} + m_{media}}{m_{sample}} \right)$$
 (5)

Calculated SAR values are listed in the table 1. The discrepancy between the SAR values obtained using the Box-Lucas Fit and those calculated with Newton's Cooling Approach arises from fundamental differences in how each method accounts for heat generation and loss during magnetic hyperthermia experiments.

In Newton's Cooling Approach, the calculation of SAR is based on the initial slope of the temperature versus time curve, assuming minimal heat losses to the environment during the early stages of heating. This method focuses on the initial rate of temperature increase and often neglects the energy lost to the surroundings throughout the experiment. As a result, it tends to underestimate the actual heat generated by the nanoparticles, leading to lower SAR values.

Comparison to Clinical Trials. When comparing the obtained SAR values of CuFe₂O₄ nanoparticles to those reported in clinical trials for magnetic hyperthermia, it is evident that the synthesized materials demonstrate promising heating efficiency. Clinical studies typically require SAR values in the range of 10–100 W/g to achieve effective tumor heating under safe magnetic field conditions (usually below 15 kA/m and 500 kHz) while

minimizing damage to surrounding healthy tissue. The CuFe₂O₄ nanoparticles studied here exhibit SAR values around 30–32 W/g (Box-Lucas fit), positioning them well within the lower-to-mid clinical range. Although iron oxide nanoparticles (e.g., Fe₃O₄) are most commonly used in clinical applications due to their established biocompatibility, the comparable SAR performance of copper ferrite, alongside its tunable magnetic properties, suggests it could serve as a viable alternative or complementary material in future hyperthermia treatments (table 2).

Further work would be required to assess their longterm biocompatibility, surface functionalization, and heating performance under in vivo conditions to fully align with clinical requirements.

Conclusions

In this work, was synthesized and systematically analyzed CuFe₂O₄ magnetic nanoparticles to evaluate their potential for magnetic hyperthermia applications. Structural characterization by XRD confirmed a phase transition from cubic (Fd3m) to tetragonal (I4₁/amd) upon annealing, while TEM revealed uniform morphology and nanoscale particle sizes. Magnetic measurements using VSM demonstrated that annealing significantly affects the saturation magnetization and coercivity, directly influencing the heating behavior under an alternating magnetic field. SAR and ILP values obtained from Box-Lucas and Newton cooling models showed that the nanoparticles exhibit efficient inductive heating, with annealed samples maintaining or slightly improving thermal performance. These findings highlight CuFe₂O₄ as a promising ferrite system for magnetothermal therapy, offering tunable properties that can be further optimized

for biomedical applications. Future work should focus on enhancing biocompatibility, in vivo performance, and clinical translation potential.

Funding:

This work was funded by the Narodowa Agencja Wymiany Akademickiej (Grant Ulam NAWA: BPN/ULM/2022/1/00093) and partly supported by Ministry of Education and Science of Ukraine, grants 24BF051-01M (0124U001654).

Acknowledgments:

The authors are grateful to the Narodowa Agencja Wymiany Akademickiej for financial support. The authors thank the Ministry of Education and Science of Ukraine for grants for implementing project 0124U001654. The authors express their sincere gratitude and respect to the Armed Forces of Ukraine, who made it possible to complete the preparation of this article for publication. The team of authors expresses their gratitude to the reviewers for valuable recommendations that have been considered to improve the quality of this paper significantly.

Mazurenko Julia – Candidate of Physical and Mathematical Sciences (Ph.D.), Research Fellow at Laboratory for Physics of Magnetic Films, G.V. Kurdyumov Institute for Metal Physics, N.A.S. of Ukraine;

Kaykan Larysa – Doctor of Physical and Mathematical Sciences, Senior Researcher at the Laboratory for Physics of Magnetic Films, G.V. Kurdyumov Institute for Metal Physics, N.A.S. of Ukraine;

Moklyak Volodymyr — Doctor of Physical and Mathematical Sciences, Professor, Head of Laboratory for Physics of Magnetic Films, G.V. Kurdyumov Institute for Metal Physics, N.A.S. of Ukraine, Professor of the Department of Physical and Mathematical Sciences, Ivano-Frankivsk National Technical University of Oil and Gas:

Moklyak Mariia – PhD Student, Department of Applied Physics and Materials Science, Vasyl Stefanyk Precarpathian National University;

Moiseienko Mykola – Doctor of Biological Sciences, Professor, Head of the Department of Medical Informatics, Medical and Biological Physics, Ivano-Frankivsk National Medical University;

Ostapovych, Nataliia – Candidate of Pedagogical Sciences (Ph.D.), Associate Professor (Docent) at the Department of Medical Informatics, Medical and Biological Physics, Ivano-Frankivsk National Medical University;

Petryshyn Mykhailo – Candidate of Technical Sciences (Ph.D.), Associate Professor (Docent) at the Department of Computer Science, Vasyl Stefanyk Precarpathian National University.

- [1] T. L. Pham, C. Q. Tong, N. P. Vu, T. H. H. Vu, T. A. Ho, D. T. Pham, T. H. Le, M. T. Dinh, T. H. Nguyen, T. K. Hoang, T. K. G. Lam, V. Nguyen, H. N. Pham, T. H. Le, Effect of Eu³⁺ion concentration on optical and magnetic properties of oriented Gd₂O₃/CTAB nanoparticles as multifunctional optical-magnetic probes in biomedicine, RSC Advances, 15(12), 9521 (2025); https://doi.org/10.1039/d5ra00932d.
- [2] S. S. Jogdand, S. S. Joshi, *Effect of polymer combustion synthesis on thermal, spectroscopic, structural, and magnetic properties of Co₃O₄ nanoparticles, Polyhedron, 269, 117419 (2025); https://doi.org/10.1016/j.poly.2025.117419.*
- [3] P. Kathiravan, K. Thillaivelavan, G. Viruthagiri, N. Shanmugam, *Investigations of thermal, structural, optical, morphological and magnetic properties of chemical precipitation synthesized NiO nanoparticles for optoelectronic applications*, Journal of the Indian Chemical Society, 101(7), 101171 (2024); https://doi.org/10.1016/j.jics.2024.101171.
- [4] W. M. da Silva, M. F. P. da Silva, R. N. de Souza, A. M. A. Silva, A. M. Rodrigues, A. S. Santos, S. da Silva, N. D. S. Mohallem, J. A. H. Coaquira, *Synthesis and characterization of few-layered carbon nanotubes decorated with magnetic nanoparticles envisaging potential technological applications*, Surfaces and Interfaces, 66, 106580 (2025); https://doi.org/10.1016/j.surfin.2025.106580.
- [5] J. Sánchez, D. A. Cortés-Hernández, P. Y. Reyes-Rodríguez, G. F. Hurtado-López, *Effect of gallium-substituted cobalt ferrites on the magnetic and crystallographic properties, heating ability and hemolytic cytotoxicity of nanoparticles synthesized by sol-gel for biomedical applications*, Ceramics International, (2025); https://doi.org/10.1016/j.ceramint.2025.02.138.
- [6] S. Pawar, N. Arepally, H. Carlton, J. Vanname, R. Ivkov, A. Attaluri, *Magnetic particle imaging resolution needed* for magnetic hyperthermia treatment planning: a sensitivity analysis, Frontiers in Thermal Engineering, 5, (2025); https://doi.org/10.3389/fther.2025.1520951.
- [7] N. Lafuente-Gómez, M. Martínez-Mingo, Z. V. Díaz-Riascos, B. García-Prats, I. de la Iglesia, M. Dhanjani, D. García-Soriano, L. A. Campos, S. Mancilla-Zamora, G. Salas, I. Abasolo, Á. Somoza, *Gemcitabine and miRNA34a mimic codelivery with magnetic nanoparticles enhanced anti-tumor effect against pancreatic cancer*, Journal of Controlled Release, 113791 (2025); https://doi.org/10.1016/j.jconrel.2025.113791.
- [8] H. Ohnishi, T. Teranishi, *Crystal Distortion in Copper Ferrite-Chromite Series*, Journal of the Physical Society of Japan, 16(1), 35 (1961); https://doi.org/10.1143/jpsj.16.35.

- [9] J. Jose, R. Kumar, S. Harilal, G. E. Mathew, D. G. T. Parambi, A. Prabhu, Md. S. Uddin, L. Aleya, H. Kim, B. Mathew, *Magnetic nanoparticles for hyperthermia in cancer treatment: an emerging tool*, Environmental Science and Pollution Research, 27(16), 19214 (2019); https://doi.org/10.1007/s11356-019-07231-2.
- [10] B. McWilliams, H. Wang, V. Binns, S. Curto, S. Bossmann, P. Prakash, *Experimental Investigation of Magnetic Nanoparticle-Enhanced Microwave Hyperthermia*, Journal of Functional Biomaterials, 8(3), 21 (2017); https://doi.org/10.3390/jfb8030021.
- [11] K. Simeonidis, E. Kaprara, P. Rivera-Gil, R. Xu, F. J. Teran, E. Kokkinos, A. Mitropoulos, N. Maniotis, L. Balcells, *Hydrotalcite-Embedded Magnetite Nanoparticles for Hyperthermia-Triggered Chemotherapy*, Nanomaterials, 11(7), 1796 (2021); https://doi.org/10.3390/nano11071796.
- [12] K. Wu, J.-P. Wang, N. A. Natekar, S. Ciannella, C. González-Fernández, J. Gomez-Pastora, Y. Bao, J. Liu, S. Liang, X. Wu, L. Nguyen T Tran, K. Mercedes Paz González, H. Choe, J. Strayer, P. R. Iyer, J. Chalmers, V. K. Chugh, B. Rezaei, S. Mostufa, M. L. Fdez-Gubieda, *Roadmap on magnetic nanoparticles in nanomedicine*, Nanotechnology, 36(4), 042003 (2024); https://doi.org/10.1088/1361-6528/ad8626.
- [13] G. Song, M. Kenney, Y.-S. Chen, X. Zheng, Y. Deng, Z. Chen, S. X. Wang, S. S. Gambhir, H. Dai, J. Rao, Carbon-coated FeCo nanoparticles as sensitive magnetic-particle-imaging tracers with photothermal and magnetothermal properties, Nature Biomedical Engineering, 4(3), 325 (2020); https://doi.org/10.1038/s41551-019-0506-0.
- [14] M.T. Luiz, J.A. P. Dutra, J.S. R. Viegas, J.T.C. de Araújo, A.G. Tavares Junior, M. Chorilli, *Hybrid Magnetic Lipid-Based Nanoparticles for Cancer Therapy*, Pharmaceutics, 15(3), 751 (2023); https://doi.org/10.3390/pharmaceutics15030751.
- [15] T.E. Torres, E. Lima Jr., M. P. Calatayud, B. Sanz, A. Ibarra, R. Fernández-Pacheco, A. Mayoral, C. Marquina, M. R. Ibarra, G. F. Goya, *The relevance of Brownian relaxation as power absorption mechanism in Magnetic Hyperthermia*, Scientific Reports, 9(1), (2019); https://doi.org/10.1038/s41598-019-40341-y.
- [16] Y. Tang, Y. Wang, R. C. C. Flesch, T. Jin, *Influence of different heat transfer models on therapeutic temperature prediction and heat-induced damage during magnetic hyperthermia*, Journal of Thermal Biology, 118, 103747 (2023); https://doi.org/10.1016/j.jtherbio.2023.103747.
- [17] C. Boitard, A. Michel, C. Ménager, N. Griffete, *Protein Denaturation Through the Use of Magnetic Molecularly Imprinted Polymer Nanoparticles*, Molecules, 26(13), 3980 (2021); https://doi.org/10.3390/molecules26133980.
- [18] X. Liu, Y. Zhang, Y. Wang, W. Zhu, G. Li, X. Ma, Y. Zhang, S. Chen, S. Tiwari, K. Shi, S. Zhang, H. M. Fan, Y. X. Zhao, X.-J. Liang, Comprehensive understanding of magnetic hyperthermia for improving antitumor therapeutic efficacy, Theranostics, 10(8), 3793 (2020); https://doi.org/10.7150/thno.40805.
- [19] Y. Liu, Z. Guo, F. Li, Y. Xiao, Y. Zhang, T. Bu, P. Jia, T. Zhe, L. Wang, *Multifunctional Magnetic Copper Ferrite Nanoparticles as Fenton-like Reaction and Near-Infrared Photothermal Agents for Synergetic Antibacterial Therapy*, ACS Applied Materials & Interfaces, 11(35), 31649 (2019); https://doi.org/10.1021/acsami.9b10096.
- [20] D. Soukup, S. Moise, E. Céspedes, J. Dobson, N. D. Telling, *In Situ Measurement of Magnetization Relaxation of Internalized Nanoparticles in Live Cells*, ACS Nano, 9(1), 231 (2015); https://doi.org/10.1021/nn503888j.
- [21] Y. Wang, Z. Chen, J. Li, Y. Wen, J. Li, Y. Lv, Z. Pei, Y. Pei, A Paramagnetic Metal-Organic Framework Enhances Mild Magnetic Hyperthermia Therapy by Downregulating Heat Shock Proteins and Promoting Ferroptosis via Aggravation of Two-Way Regulated Redox Dyshomeostasis, Advanced Science, 11(11), (2023); https://doi.org/10.1002/advs.202306178.
- [22] J. Mazurenko, A. K. Sijo, L. Kaykan, V. Kotsyubynsky, Ł. Gondek, A. Zywczak, M. Marzec, O. Vyshnevskyi, *Synthesis and Characterization of Copper Ferrite Nanoparticles for Efficient Photocatalytic Degradation of Organic Dyes*, Journal of Nanotechnology, 2025(1), (2025); https://doi.org/10.1155/jnt/8899491.
- [23] L. S. Kaykan, J. S. Mazurenko, N. V. Ostapovych, A. K. Sijo, N. Ya. Ivanichok, Effect of pH on Structural Morphology and Magnetic Properties of Ordered Phase of Cobalt Doped Lithium Ferrite Nanoparticles Synthesized by Sol-gel Auto-combustion Method, Journal of Nano- and Electronic Physics, 12, 04008 (2020); https://doi.org/10.21272/jnep.12(4).04008
- [24] J. Mazurenko, L. Kaykan, J. M. Michalik, M. Sikora, E. Szostak, O. Vyshnevskyi, K. Bandura, L. Turovska, Enhanced Synthesis of Copper Ferrite Magnetic Nanoparticles via Polymer-Assisted Sol-Gel Autocombustion Method for Magnetic Hyperthermia Applications, Journal of Nano Research, 84, 95 (2024); https://doi.org/10.4028/p-jbv1le.
- [25] D. Lachowicz, W. Górka, A. Kmita, A. Bernasik, J. Żukrowski, W. Szczerba, M. Sikora, C. Kapusta, S. Zapotoczny, *Enhanced hyperthermic properties of biocompatible zinc ferrite nanoparticles with a charged polysaccharide coating*, Journal of Materials Chemistry B, 7(18), 2962 (2019); https://doi.org/10.1039/c9tb00029a.
- [26] B. K. Ostafiychuk, L. S. Kaykan, J. S. Mazurenko, B. Ya. Deputat, S. V. Koren, *Effect of substitution on the mechanism of conductivity of ultra dispersed lithium–iron spinel, substituted with magnesium ions*, Journal of Nanoand Electronic Physics, 9, 05018 (2017); https://doi.org/10.21272/jnep.9(5).05018
- [27] J. Mazurenko, L. Kaykan, A. Zywczak, V. Kotsyubynsky, Kh. Bandura, M. Moiseienko, A. Vytvytskyi, *Study of Li-Al Ferrites by Nuclear Magnetic Resonance, UV-Spectroscopy, and Mossbauer Spectroscopy*, Journal of Nanoand Electronic Physics, 15(2), 02020 (2023); https://doi.org/10.21272/jnep.15(2).02020.
- [28] O.L. Lanier, O.I. Korotych, A.G. Monsalve, D.Wable, S. Savliwala, N. W. F. Grooms, C. Nacea, O. R. Tuitt, J. Dobson, *Evaluation of magnetic nanoparticles for magnetic fluid hyperthermia*, International Journal of Hyperthermia, 36(1), 686 (2019); https://doi.org/10.1080/02656736.2019.1628313.

- [29] B. B. Lahiri, S. Ranoo, J. Philip, Effect of orientational ordering of magnetic nanoemulsions immobilized in agar gel on magnetic hyperthermia, Journal of Magnetism and Magnetic Materials, 451, 254 (2018); https://doi.org/10.1016/j.jmmm.2017.10.068.
- [30] D. Serantes, K. Simeonidis, M. Angelakeris, O. Chubykalo-Fesenko, M. P. Marciello, M. del P. Morales, D. Baldomir, C. Martinez-Boubeta, *Multiplying Magnetic Hyperthermia Response by Nanoparticle Assembling*, The Journal of Physical Chemistry C, 118(11), 5927 (2014); https://doi.org/10.1021/jp410717m.
- [31] M. Kallumadil, M. Tada, T. Nakagawa, M. Abe, P. Southern, Q. A. Pankhurst, *Suitability of commercial colloids* for magnetic hyperthermia, Journal of Magnetism and Magnetic Materials, 321(10), 1509 (2009); https://doi.org/10.1016/j.jmmm.2009.02.075.
- [32] F. J. Teran, C. Casado, N. Mikuszeit, G. Salas, A. Bollero, M. P. Morales, J. Camarero, R. Miranda, *Accurate determination of the specific absorption rate in superparamagnetic nanoparticles under non-adiabatic conditions*, Applied Physics Letters, 101(6), 062413 (2012); https://doi.org/10.1063/1.4742918.
- [33] K. Murase, H. Takata, Y. Takeuchi, S. Saito, Control of the temperature rise in magnetic hyperthermia with use of an external static magnetic field, Physica Medica, 29(6), 624 (2013); https://doi.org/10.1016/j.ejmp.2012.08.005.
- [34] P. T. Phong, P. H. Nam, D. H. Manh, I.-J. Lee, $Mn_{0.5}Zn_{0.5}Fe_2O_4$ nanoparticles with high intrinsic loss power for hyperthermia therapy, Journal of Magnetism and Magnetic Materials, 433, 76 (2017); https://doi.org/10.1016/j.jmmm.2017.03.001.
- [35] S. Ruta, Y. Fernández-Afonso, S. E. Rannala, M. P. Morales, S. Veintemillas-Verdaguer, C. Jones, L. Gutiérrez, R. W. Chantrell, D. Serantes, *Beyond Newton's law of cooling in evaluating magnetic hyperthermia performance: a device-independent procedure*, Nanoscale Advances, 6(16), 4207 (2024); https://doi.org/10.1039/d4na00383g.
- [36] N. Rmili, K. Riahi, R. M'nassri, B. Ouertani, W. Cheikhrouhou-Koubaa, E. K. Hlil, *Magnetocaloric and induction heating characteristics of La_{0.71}Sr_{0.29}Mn_{0.95}Fe_{0.05}O₃ nanoparticles, Journal of Sol-Gel Science and Technology, (2024); https://doi.org/10.1007/s10971-024-06361-5.*
- [37] V. Manescu (Paltanea), I. Antoniac, G. Paltanea, I. V. Nemoianu, A. G. Mohan, A. Antoniac, J. V. Rau, S. A. Laptoiu, P. Mihai, H. Gavrila, A. R. Al-Moushaly, A. D. Bodog, *Magnetic Hyperthermia in Glioblastoma Multiforme Treatment*, International Journal of Molecular Sciences, 25(18), 10065 (2024); https://doi.org/10.3390/ijms251810065.
- [38] H. A. Elkayal, N. E. Ismail, Efficient focusing of microwave hyperthermia for small deep-seated breast tumors treatment using particle swarm optimization, Computer Methods in Biomechanics and Biomedical Engineering, 24(9), 985 (2021); https://doi.org/10.1080/10255842.2020.1863379.
- [39] N. Yoshikawa, Y. Itoh, T. Matsukawa, M. Kawamura, K. Yamada, S. Nakamura, H. Kajiyama, *Local hyperthermia with built-in endoscopy for radioresistant cervical cancer: a case series*, Nagoya Journal of Medical Science, 85(3), 639 (2023); https://doi.org/10.18999/nagjms.85.3.639.
- [40] J. Cohen, A. Anvari, S. Samanta, Y. Poirier, S. Soman, A. Alexander, M. Ranjbar, R. Pavlovic, A. Zodda, I. L. Jackson, J. Mahmood, Z. Vujaskovic, A. Sawant, *Mild hyperthermia as a localized radiosensitizer for deep-seated tumors: investigation in an orthotopic prostate cancer model in mice*, The British Journal of Radiology, 92(1095), 20180759 (2019); https://doi.org/10.1259/bjr.20180759.
- [41] L. Shoshiashvili, I. Shamatava, D. Kakulia, F. Shubitidze, *Design and Assessment of a Novel Biconical Human-Sized Alternating Magnetic Field Coil for MNP Hyperthermia Treatment of Deep-Seated Cancer*, Cancers, 15(6), 1672 (2023); https://doi.org/10.3390/cancers15061672.
- [42] O. Kaidar-Person, S. Oldenborg, P. Poortmans, *Re-irradiation and Hyperthermia in Breast Cancer*, Clinical Oncology, 30(2), 73 (2018); https://doi.org/10.1016/j.clon.2017.11.004.
- [43] S. Gao, M. Zheng, X. Ren, Y. Tang, X. Liang, Local hyperthermia in head and neck cancer: mechanism, application and advance, Oncotarget, 7(35), 57367 (2016); https://doi.org/10.18632/oncotarget.10350.
- [44] X. Gao, Y. Zhang, X. Han, Z. Li, B. Chen, Q. Li, L. Hu, Y. Lv, F. Ren, *Numerical analysis and animal study of noninvasive handheld electroporation delivery device for skin superficial lesion treatment*, International Journal of Hyperthermia, 39(1), 1017 (2022); https://doi.org/10.1080/02656736.2022.2104937.
- [45] N. Pyrgidis, M. Chaloupka, B. Ebner, Y. Volz, P. Weinhold, J. Marcon, L. Eismann, C. G. Stief, G. B. Schulz, M. Apfelbeck, Perioperative complications of focal therapy for prostate cancer: results from the GeRmAn Nationwide inpatient Data (GRAND) study, BJU International, (2025); https://doi.org/10.1111/bju.16746.
- [46] H. Chan, H.-Y. Chang, W.-L. Lin, G.-S. Chen, Large-Volume Focused-Ultrasound Mild Hyperthermia for Improving Blood-Brain Tumor Barrier Permeability Application, Pharmaceutics, 14(10), 2012 (2022); https://doi.org/10.3390/pharmaceutics14102012.
- [47] L. Yan, H. Huang, J. Lin, R. Yu, *High-intensity focused ultrasound treatment for symptomatic uterine fibroids:* a systematic review and meta-analysis, International Journal of Hyperthermia, 39(1), 230 (2022); https://doi.org/10.1080/02656736.2022.2029956.
- [48] C. Kim, Y. Guo, A. Velalopoulou, J. Leisen, A. Motamarry, K. Ramajayam, M. Aryal, D. Haemmerich, C. D. Arvanitis, Closed-loop trans-skull ultrasound hyperthermia leads to improved drug delivery from thermosensitive drugs and promotes changes in vascular transport dynamics in brain tumors, Theranostics, 11(15), 7276 (2021); https://doi.org/10.7150/thno.54630.
- [49] D. Chen, Y. Tang, J. Zhu, J. Zhang, X. Song, W. Wang, J. Shao, W. Huang, P. Chen, X. Dong, *Photothermal-pH-hypoxia responsive multifunctional nanoplatform for cancer photo-chemo therapy with negligible skin phototoxicity*, Biomaterials, 221, 119422 (2019); https://doi.org/10.1016/j.biomaterials.2019.119422.

- [50] Y. Zhang, F. Li, S. Ya, Y. Hu, D. Zhi, W. Wang, M. Xu, B. Qiu, W. Ding, *An iron oxide nanoparticle-based transdermal nanoplatform for dual-modal imaging-guided chemo-photothermal therapy of superficial tumors*, Acta Biomaterialia, 130, 473 (2021); https://doi.org/10.1016/j.actbio.2021.05.033.
- [51] S. Hao, H. Han, Z. Yang, M. Chen, Y. Jiang, G. Lu, L. Dong, H. Wen, H. Li, J. Liu, L. Wu, Z. Wang, F. Wang, Recent Advancements on Photothermal Conversion and Antibacterial Applications over MXenes-Based Materials, Nano-Micro Letters, 14(1), (2022); https://doi.org/10.1007/s40820-022-00901-w.
- [52] T. Du, Z. Xiao, G. Zhang, L. Wei, J. Cao, Z. Zhang, X. Li, Z. Song, W. Wang, J. Liu, X. Du, S. Wang, *An injectable multifunctional hydrogel for eradication of bacterial biofilms and wound healing*, Acta Biomaterialia, 161, 112 (2023); https://doi.org/10.1016/j.actbio.2023.03.008.

Ю. Мазуренко 1,2 , Л. Кайкан 1 , В. Мокляк 1,3 , М. Мокляк 4 , М. Мойсеєнко 5 , Н. Остапович 5 , М. Петришин 6

Індукційні теплові властивості магнітних наночастинок мідного фериту

¹Лабораторія фізики магнітних плівок №23, Інститут металофізики ім. Г.В. Курдюмова НАН України, Київ, Україна; ²Відділ магнетизму, Інститут експериментальної фізики Словацької академії наук, Кошиці, Словацька Республіка, <u>mazurenko@saske.sk</u>;

³Кафедра фізико-математичних наук, Івано-Франківський національний технічний університет нафти і газу, Івано-Франківськ, Україна, <u>volodymyr.mokliak@nung.edu.ua</u>;

⁴Кафедра прикладної фізики і матеріалознавства, Прикарпатський національний університет ім. Василя Стефаника, Івано-Франківськ, Україна, <u>mariamoklyak@gmail.com;</u>

⁵Кафедра медичної інформатики, медичної та біологічної фізики, Івано-Франківський національний медичний університет, Івано-Франківськ, Україна, <u>mmoiseyenko@ifnmu.edu.ua</u>, <u>nataost@ifnmu.edu.ua</u>;

⁶Кафедра комп'ютерних наук, Прикарпатський національний університет ім. Василя Стефаника, Івано-Франківськ, Україна, m.l.petryshyn@pnu.edu.ua

У цьому дослідженні розглянуто індукційні властивості нагрівання магнітних наночастинок CuFe₂O₄ (МНЧ) для потенційного застосування в магнітній гіпертермії. Наночастинки CuFe₂O₄ були синтезовані методом соль-гель автогоріння та піддані відпалу при 400°С і 800°С для оцінки впливу термообробки на їхні структурні та магнітні властивості. Рентгенівський фазовий аналіз (XRD) показав фазовий перехід від кубічної шпінельної структури (Fd3m) у вихідних зразках до тетрагональної фази (I4₁/amd) після відпалу, при цьому розмір частинок складав 20–30 нм. Аналіз за допомогою просвічуючої електронної мікроскопії (ПЕМ) підтвердив сферичну морфологію та однорідний розподіл частинок, а вимірювання на вібраційному магнітометрі (VSM) показали, що відпал істотно впливає на намагніченість насичення та коерцитивну силу – ключові параметри для ефективності нагрівання. Питома швидкість поглинання (SAR) та питомі втрати (ILP), оцінені за моделями Бокса-Лукаса та охолодження Ньютона, показали, що наночастинки зберігають високу ефективність нагрівання після термічної обробки, з SAR ~30–32 Вт/г. Результати свідчать, що наночастинки CuFe₂O₄ є перспективними кандидатами для магнітно керованої гіпертермії з можливістю оптимізації їх властивостей для клінічного використання.

Ключові слова: мідний ферит, магнітні наночастинки, індукційне нагрівання, метод Бокса-Лукаса, підхід охолодження Ньютона.